

## Validation Study

# Correlation Between a Novel Surface Topography Asymmetry Analysis and Radiographic Data in Scoliosis

Amin Komeili, MSc<sup>a</sup>, Lindsey Westover, MSc<sup>b,\*</sup>, Eric C. Parent, PhD<sup>c</sup>, Marwan El-Rich, PhD<sup>a</sup>, Samer Adeeb, PhD<sup>a</sup>

<sup>a</sup>Department of Civil and Environmental Engineering, University of Alberta, Edmonton, Alberta T6G2V4, Canada

<sup>b</sup>Department of Mechanical Engineering, University of Alberta, Edmonton, Alberta T6G2G8, Canada

<sup>c</sup>Department of Physical Therapy, Faculty of Rehabilitation Medicine, University of Alberta, Edmonton, Alberta T6G2G4, Canada

Received 5 May 2014; revised 17 December 2014; accepted 2 February 2015

## Abstract

**Study Design:** Cross-sectional study.

**Objective:** To investigate the correlation between parameters extracted from a three-dimensional (3D) asymmetry analysis of the torso and the internal deformities of the spine presented on radiographs, including 1) curve number, direction and location; 2) location of the apical vertebra; and 3) curve severity.

**Summary of Background Data:** Surface topography (ST) is used to assess external torso deformities and may predict important characteristics of the underlying spinal curves. ST does not expose patients to radiation and could safely be used clinically for scoliosis patients. Most ST indices rely on anatomical landmarks on the torso and 2D measurements.

**Methods:** The ability of a 3D markerless asymmetry technique to predict radiographic characteristics was assessed for 100 scoliosis patients with full torso ST scans. Twenty-four additional patients were used for validation. The number, direction, and location of curves were determined by three examiners using ST deviation color maps. The inter-method percentage of agreement and Kappa coefficient were estimated for each measure. Linear regression predicted the vertical location of the apical vertebra from ST. Curve severity (mild, moderate, severe) was predicted with a decision tree analysis using ST parameters.

**Results:** The average percentage of agreement was 62%, 66%, and 23% for single, double, and triple curves, respectively. Curve direction was always correctly identified. The average percentages of agreement for curve location were 63%, 92%, and 62% for proximal thoracic, thoracic/thoracolumbar (T-TL), and lumbar (L) curves, respectively. Apical vertebra location was predicted with  $R^2 = 0.89$  for T-TL and  $R^2 = 0.58$  for L curves. ST parameters classified curve severity for T-TL and L curves with 73% and 59% accuracy, respectively.

**Conclusions:** The method presented here improves upon current ST techniques by using the entire torso surface and both a visual and quantitative representation of the asymmetry to better capture the torso deformity.

© 2015 Scoliosis Research Society.

**Keywords:** Surface topography; Asymmetry analysis; Adolescent idiopathic; Scoliosis; Radiography

## Introduction

Spinal deformities such as scoliosis affect both internal and external alignment and vary among patients [1]. It is

important to monitor the scoliosis deformity with regular clinical visits in order to identify progression and prescribe appropriate treatments. The Cobb angle measured on posterior-anterior (PA) radiographs is the standard to monitor scoliosis [2–5].

Mild curves (Cobb angle  $< 25^\circ$ ) typically do not require treatment. Moderate curves (Cobb angle between  $25^\circ$  and  $40^\circ$ ) are treated using noninvasive methods such as bracing. Severe curves (Cobb angle  $> 40^\circ$  or  $50^\circ$ ) may require spinal fusion and instrumentation surgery to correct the curve [6].

Using the Cobb angle in monitoring scoliosis is problematic because of the long-term effects of radiation [7–10], including an increase in the risk for breast cancer [11].

Author disclosures: AK (none); LW (none); ECP (grants from the Women and Children Health Research Institute [Stollery] and the Scoliosis Research Society, during the conduct of the study); ME (none); SA (grants from the Scoliosis Research Society and the Natural Sciences and Engineering Research Council of Canada, during the conduct of the study).

\*Corresponding author. 6-23 Mechanical Engineering Building, University of Alberta, Edmonton, Alberta, Canada T6G 2G8. Tel.: +1 780 492 3598; fax: +1 780 492 2200.

E-mail address: lwestove@ualberta.ca (L. Westover).

Additionally, because the Cobb angle is measured from two-dimensional radiographs, it has a limited ability to fully describe the three-dimensional (3D) spinal deformities associated with scoliosis. Moreover, the cosmetic appearance of the torso is a major concern of patients, which cannot be captured with radiographs [12,13].

Surface topography (ST) has been suggested to assess the deformities associated with scoliosis [12,14–20]. Attempts have been made to use ST to predict the Cobb angle and the geometry of the underlying spine in order to replace or decrease the periodic radiographic evaluations [12,16,20–27]. However, most of the current ST methods assess the torso deformities by measuring indices from manually placed markers [12,14,26,28]. Marker placement requires a trained operator and can introduce measurement error and uncertainties. Additionally, the number and location of anatomical landmarks are limited, and the 3D torso surface cannot be fully represented by so few points.

A novel 3D markerless ST technique has been recently developed to identify areas and patterns of asymmetry using the “best plane of symmetry” [29]. Torso asymmetries are illustrated using a deviation color map (DCM) on the 3D model of the patient’s torso. Because the indices are extracted without human intervention, the issues with marker placement are avoided. The proposed asymmetry measures are universal and independent of the scanning technology employed. Previously, patients have been reliably classified into various groups according to their DCM [29]. In the present study, the clinical relevance and relation of the DCMs to radiographic measures of scoliosis is studied.

The objectives of this study are to determine the ability of the asymmetry analysis to 1) identify the number, direction, and location of scoliosis curves; 2) predict the vertical height of the curve apex; and 3) predict the curve severity, defined as mild (Cobb angle  $<25^\circ$ ), moderate ( $25^\circ < \text{Cobb angle} < 40^\circ$ ), and severe (Cobb angle  $>40^\circ$ ). The long-term objective of this work is to develop noninvasive methods based on ST analysis to accurately quantify and monitor scoliosis deformities with the aim of reducing the number of required x-rays.

## Materials and Methods

Torso scans from 100 patients with adolescent idiopathic scoliosis (AIS) were selected randomly from scans collected in an ongoing study on full-torso ST (Table 1a). All subjects had no surgical treatment and had an ST scan with a corresponding radiograph. Data were collected from consenting volunteers during routine clinical visits. Ethics approval from the human research ethics board was obtained.

Torso scans of 24 additional patients with AIS (Table 1b) meeting the same selection criteria were employed as a validation sample to assess the accuracy of the model developed for predicting the location of the curve apex from ST data.

Table 1

Description of subjects (a) test subjects (b) validation sample.

(a) Test subjects		(b) Validation sample	
Total subjects	100	Total subjects	24
Age, years	10–18	Age, years	10–18
Cobb angle, $^\circ$	$10^\circ$ – $69^\circ$	Cobb angle, $^\circ$	$12^\circ$ – $63^\circ$
Gender, n		Gender, n (%)	
Male	22	Male	5 (20.8)
Female	78	Female	19 (79.2)
Curve type, n		Curve type, n (%)	
Lenke 1	32	Lenke 1	8 (33.3)
Lenke 2	3	Lenke 2	0
Lenke 3	13	Lenke 3	3 (12.5)
Lenke 4	0	Lenke 4	2 (8.3)
Lenke 5	46	Lenke 5	9 (37.5)
Lenke 6	6	Lenke 6	2 (8.3)

## Data Collection

ST data were collected using four Minolta scanners to capture the front, back, and side views of the torso surface [30], which were merged to reconstruct the 3D model of the torso. Asymmetry was investigated using our previously developed 3D markerless asymmetry analysis [29]. The torso was reflected about the best plane of symmetry and was compared with its reflection to identify the areas of asymmetry in the form of a DCM. Based on our previous work, deviation  $<3$  mm was considered normal [29]. Any deviation  $>3$  mm was shown with a red or blue color depending on whether the asymmetry was convex (blue) or concave (red) relative to the other side of the torso. When viewing the DCM from the back of the patient, the pattern of color patches is symmetric about the best plane of symmetry (approximately midsagittal), with each blue-colored patch having a corresponding red-colored patch on the other side of the torso (Fig. 1A). To quantify the local deformities, the color patches were automatically isolated from the DCM. Because of symmetry, only one side of the torso was used to calculate the quantitative parameters from the DCM. Figure 1 shows an example of the DCM and the isolated color patches.

All subjects received a PA radiograph as part of their routine clinical visit. Radiographs were taken the same day and in a similar position as the ST images, and served as the gold standard to assess the performance of the predictions from the ST data.

### Number, direction, and location of curves

Three novice observers determined the number, direction, and location of the curve(s) from the DCM. The novice observers were graduate and undergraduate engineering students conducting research in our institution. Standard instructions were provided by the author. The observers first counted the number of color patches in the DCM. To determine the direction of the curve, observers simply determined if the blue color was on the right or left side of

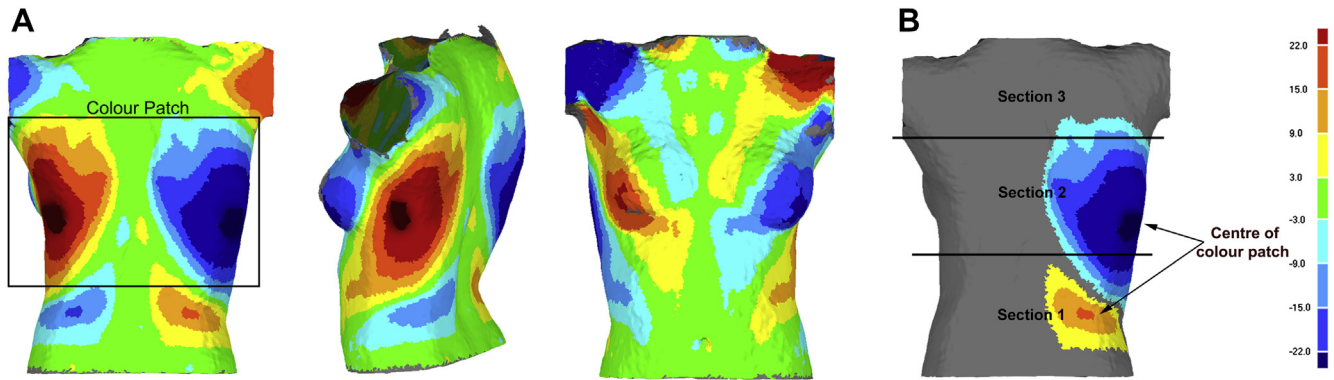


Fig. 1. (A) Full deviation color map (DCM) of an analyzed torso from back, side, and front view. (B) color patches isolated from the DCM.

Table 2  
Determining the location of curve (T-TL, L) based on the subgroup category.

Subgroup	Location of the colour patch center (see Fig. 1B)	Curve location
1	Section 2	T-TL
	Section 3	PT
2	Section 1	L
3	Section 2	T-TL
4, 6	Section 1	L
	Section 2	T-TL
	Section 3	PT
5	Section 1	L
	Section 2	T-TL

T-TL, thoracic/thoracolumbar; PT, proximal thoracic; L, lumbar.

the torso. Finally, the height of the torso was equally divided into three sections (visually) and observers identified the section in which the center of the color patch was located. The curve location was classified as lumbar (L), thoracic/thoracolumbar (T-TL), or proximal thoracic (PT) based on our previous work [29]. Table 2 summarizes this procedure using the subgroups defined by Komeili et al. [29].

Each measure was compared with the clinical data to investigate the intermethod reliability between the DCMs and the radiographs. All radiographic measurements were collected by clinicians in our scoliosis clinic. The intermethod percentage of agreement (P%) and kappa coefficient were calculated for each observer. The analysis was repeated for a subset of subjects with Cobb angles greater than 25°, which corresponds to a group with clinically important curves where bracing is usually recommended.

#### Height of the curve apex

The vertical distance between the center of each color patch (point with maximum deviation) and the posterior superior iliac spine (PSIS) was measured in the DCM and termed  $h_{st}$  (Fig. 2A). From the corresponding radiograph, the vertical distance between the center of the apical

vertebra and the PSIS was measured using the calibrated axis in the radiograph and termed  $h_r$  (Fig. 2B.)

The 100-subject cohort was used to develop a linear regression model of the form

$$h_r = Ah_{st} + B$$

The correlation between  $h_r$  and  $h_{st}$  was assessed using the coefficient of determination ( $R^2$ ) obtained from the linear regression model. It should be noted that the  $R^2$  value has a range from 0 to 1, with a value of 1 indicating a perfect fit between the data and the model. The  $R^2$  value can also be interpreted as the proportion of variance in the predicted outcome explained by the regression model. The 24-subject cohort was used as a validation sample to assess the accuracy of the model. The analysis was repeated for the subset of subjects with Cobb angles greater than 25°.

#### Curve magnitude

The DCM represents the distance between the original torso and the reflected torso. Each point in the original torso has a corresponding closest point in the reflected torso. The individual point-by-point deviation is the distance between one point on the original torso and its corresponding point on the reflected torso. For an isolated color patch, the maximum deviation and root mean square of the individual point-by-point deviation were chosen as independent parameters to predict curve severity. A decision tree analysis was developed with Matlab (release 2012b, MathWorks Inc., 2012) using these measures to classify each curve into the following groups: severe (Cobb angle > 40°), moderate (25° < Cobb angle < 40°), and mild (Cobb angle < 25°). Curves were divided into T-TL and L groups based on the radiographs, and the decision tree analysis was performed separately for each group because lateral deformation of a T-TL curve is transferred to the trunk surface differently via the rib cage compared to an L curve. The surface predictions were tabulated against radiographic data, and the accuracy of the classification was estimated.

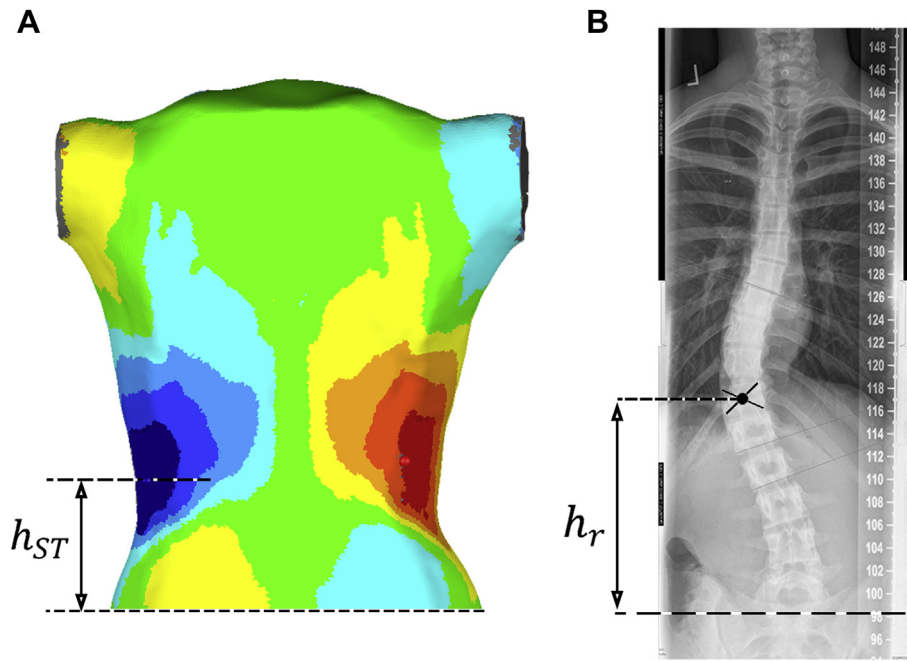


Fig. 2. (A) Vertical distance between the point with maximum deviation and posterior superior iliac spine (PSIS) measured from the deviation color map. (B) vertical distance between apical vertebra and PSIS measured using corresponding radiograph.

Results

The average time to crop the arms, head, and frame components was less than 2 minutes (29). The running time to obtain the DCM of the torso from the point cloud and determine the ST parameters, using a desktop computer equipped with a core i7 processor and 16 gigabytes of memory, was between 10 and 15 minutes, depending on the number of points in the torso model. Torso models in our sample contained at least 25,000 data points.

Table 3 shows the number and distribution of subjects in both the development and validation samples based on the location of curve and magnitude of the Cobb angle. Investigating 100 radiographs of patients with AIS as a development sample resulted in 20 PT, 102 T-TL, and 34 L curves, respectively. The validation sample contained 24 subjects with 4 PT, 25 T-TL, and 11 L curves. Because some of the subjects had double or triple curves, the number of curves exceeds the number of subjects in both samples.

Table 4 shows the number of true and false predictions for counting the number of curves and identifying the location of curves. Table 5 shows the P% and kappa coefficient for determining the number and location of the curves from the DCMs. It should be noted that the false predictions in Table 4 include both false positive and false negative predictions. However, only the true predictions contribute to the P% and kappa coefficient values shown in Table 5.

Considering the number of curves, on average, 27, 31, and 2 curves were correctly classified as single, double, and triple curves, respectively. These correspond to P% values of 62%, 66%, and 23% and a kappa coefficient of 0.32. Improved agreement was observed when mild curves were excluded (58 cases), with P% values of 72%, 77%, and 0% for single, double, and triple curves, respectively, and a kappa coefficient of 0.52.

Considering the location of curves, 13, 93, and 21 curves were correctly identified as PT, T-TL, and L

Table 3  
Distribution of the curves based on the location of curve and Cobb angle value.

	Location of curve	Mild: Cobb angle <25°	Moderate: 25° < Cobb < 40°	Severe: 40° < Cobb	Total
Development sample (n = 100)	PT	15 (10)	3 (2)	2 (1)	20
	T-TL	45 (29)	33 (21)	24 (15)	102
	L	14 (9)	12 (8)	8 (5)	34
Validation sample (n = 24)	PT	1 (3)	2 (5)	1 (3)	4
	T-TL	11 (28)	10 (25)	4 (10)	25
	L	3 (8)	6 (15)	2 (5)	11

PT, proximal thoracic; T-TL, thoracic/thoracolumbar; L, lumbar.  
Values are n (%).



Table 4

The observers' classification of the number and location of the curves.

Observer	Number of curves						Location of curves					
	Single (n = 43)		Double (n = 47)		Triple (n = 10)		PT (n = 20)		T-TL (n = 102)		L (n = 34)	
	T	F	T	F	T	F	T	F	T	F	T	F
1	26	25	31	38	3	14	16	25	96	12	20	31
2	24	28	35	34	2	15	11	24	98	10	21	37
3	30	29	27	37	2	14	11	22	86	22	22	36
Average	27	27	31	36	2	14	13	24	93	15	21	35

Observer	Number of curves with Cobb angle > 25°						Location of curves with Cobb angle > 25°					
	Single (n = 19)		Double (n = 22)		Triple (n = 1)		PT (n = 5)		T-TL (n = 57)		L (n = 20)	
	T	F	T	F	T	F	T	F	T	F	T	F
1	13	6	16	12	0	6	5	15	55	3	14	14
2	14	6	18	9	0	4	4	10	55	3	13	18
3	14	8	17	10	0	3	4	9	52	6	14	16
Average	14	7	17	10	0	4	4	11	54	4	14	16

T, true; F, false (false positive + false negative).

Values are n.

Table 5

Percentage of agreement (P%) and measure of agreement coefficient (kappa) between the observers classification and radiograph measurements.

Observer	Number of curves					Location of curves				
	Single	Double	Triple	Kappa	95% CI	PT	T-TL	L	Kappa	95% CI
	(n = 43), P%	(n = 47), P%	(n = 10), P%			(n = 20), P%	(n = 102), P%	(n = 34), P%		
1	60	66	30	0.32	0.16–0.48	80	94	59	0.72	0.64–0.81
2	56	74	20	0.33	0.17–0.49	55	96	62	0.70	0.61–0.79
3	72	57	20	0.30	0.14–0.45	55	84	65	0.60	0.51–0.70
Average	62	66	23	0.32		63	92	62	0.67	

Observer	Number of curves with Cobb angle > 25°					Location of curves with Cobb angle > 25°				
	Single	Double	Triple	Kappa	95% CI	PT	T-TL	L	Kappa	95% CI
	(n = 19), P%	(n = 22), P%	(n = 1), P%			(n = 5), P%	(n = 57), P%	(n = 20), P%		
1	68	73	0	0.47	0.25–0.69	100	96	70	0.78	0.66–0.90
2	74	82	0	0.57	0.35–0.79	80	96	65	0.74	0.61–0.86
3	74	77	0	0.52	0.28–0.75	80	91	70	0.70	0.57–0.83
Average	72	77	0	0.52		87	95	68	0.74	

curves, respectively. These predictions correspond to P% values of 63%, 92%, and 62%, respectively, and a kappa coefficient of 0.67. Again, improved agreement was observed when mild curves were excluded, with P% values of 87%, 95%, and 68% for PT, T-TL, and L curves, respectively, and a kappa coefficient of 0.74. Curve direction was predicted with 100% agreement when a scoliosis curve was present.

Figure 3A compares the vertical location of the apical vertebra measured from radiographs ( $h_r$ ) and DCMs ( $h_{ST}$ ). The coefficient of determination ( $R^2$  value) was used to indicate how well the data fit the developed predictive models. The predictive model for T-TL curves was  $h_r = 0.90h_{ST} + 69.80$  with an  $R^2$  value of 0.78. The predictive model for L curves was  $h_r = 0.80h_{ST} + 60.53$  with an  $R^2$  value of 0.51. The majority of outliers were found to represent mild curves. In Fig. 3B, mild curves (44 T-TL and 13 L curves) were excluded from the regression analysis, and the  $R^2$  values increased to 0.83 (predictive model:  $h_r = 1.05h_{ST} + 45.44$ )

and 0.61 (predictive model:  $h_r = 0.87h_{ST} + 50.37$ ) for T-TL and L curves, respectively.

The models developed for the full range of curves (Fig. 3A) were validated with an additional cohort of 24 subjects.  $h_r$  was predicted with 89% accuracy for T-TL curves and 58% accuracy for L curves based on  $R^2$  values (Fig. 3C). The average difference between the predicted value and the measured value for T-TL and L curves was 17 mm and 13 mm, respectively.

Figure 4 shows the decision trees that were developed to identify the severity for the T-TL and L curves from the DCM data along with the results of the prediction. Based on the top table in Fig. 4, the accuracy of prediction for T-TL curves was 73% (74/102), with 32/45 mild curves classified correctly (71%), 22/33 moderate curves (67%), and 20/24 severe curves (83%). The bottom table in Fig. 4 represents the detail of curve severity classification for L curves. The accuracy of prediction for L curves was 59% (20/34), with 7/14 mild curves classified correctly (50%),

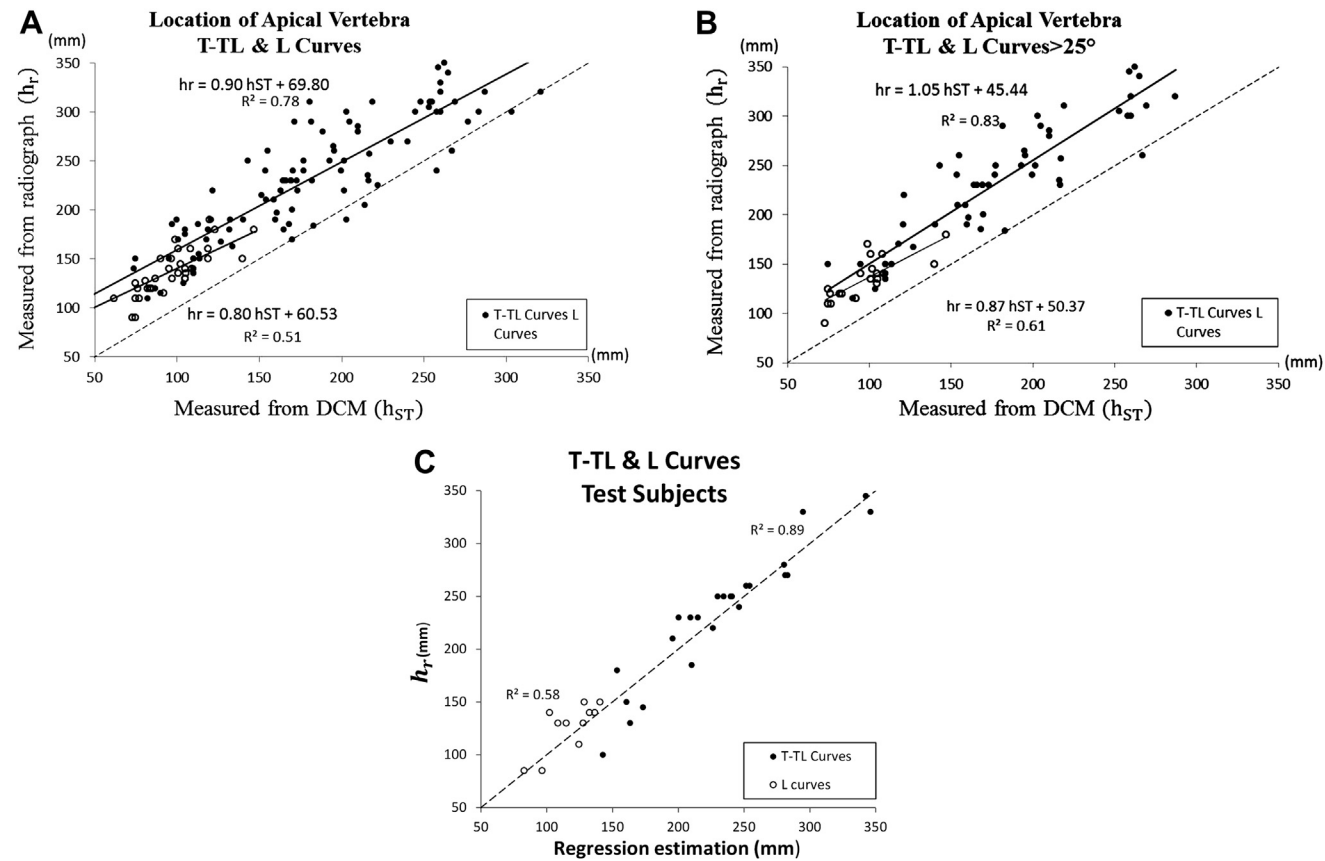


Fig. 3. The prediction of the location of apical vertebra using the vertical position of the point with maximum deviation in the color patch: (A) 102 T-TL and 34 L curves, (B) 57 T-TL and 20 L curves with Cobb angle > 25°, (C) 24 validation sample subjects using regression line.

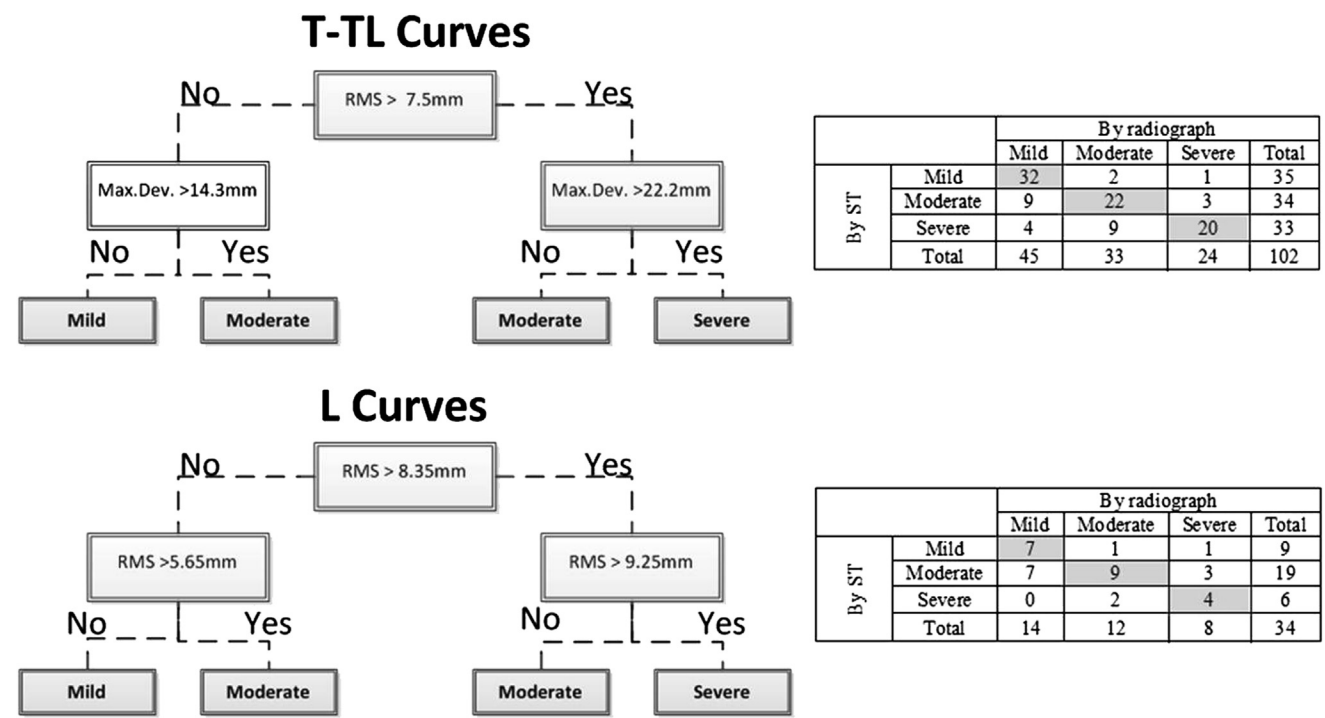


Fig. 4. Classification trees to identify the degree of scoliosis using root mean square (RMS) and maximum deviation (Max. Dev.) of the color patch for T-TL and L curves.

9/12 moderate curves (75%), and 4/8 severe curves (50%). Interestingly, the results showed that 95% of T-TL curves and 90% of L curves were correctly classified when the moderate and severe groups were combined and contrasted with the mild group.

## Discussion

This study presents an ST technique for identifying torso surface asymmetries associated with scoliosis and develops the correlation between the ST measures and clinically relevant radiographic parameters. DCMs were used to predict the number, direction, and location of curves, estimate the height of the apical vertebra, and predict the curve severity for a cohort of subjects with scoliosis. The developed procedure is quick, reliable, and does not require manual intervention.

The kappa coefficient was poor when observers counted the number of curves. This is because observers often counted extra curves, mostly PT, from the DCMs. Twenty-one color patches were identified on the shoulders (Section 3), where there were no curves on the corresponding radiograph. Axial rotation of the torso or uneven shoulders may have produced color patches in the PT region in the absence of a scoliosis curve. Similarly, the upper torso may be rotated because of the rotation within a scoliosis curve located lower. In the future, developing a scanning procedure controlling shoulder rotation and involving a lateral glide of the scapulae to expose the upper rib cage and spine may improve the ability of asymmetry analysis to detect upper curves. Less than 10% of curves were missed, mostly mild curves for which the corresponding color patch was small. Excluding mild curves increased the average agreement to 72% and 77% for identifying the number of single and double curves. A small curve typically exhibits a small torso deformity, leading to scattered color patches on the DCM. These patches are more difficult to identify than the clear color patches associated with larger curves.

The direction of the curve was identified on the DCM with 100% accuracy. This indicates that this aspect of the spinal deformity translates to a torso surface deformity in a predictable manner, that is, a right curve produces an outward protrusion on the right side of the back and a left curve produces an outward protrusion on the left side of the back.

When predicting the location of the curve, T-TL curves were identified with excellent accuracy ( $P\% = 92\%$ ), whereas PT and L curves were identified with 63% and 62% accuracy, respectively (Table 5). Excluding mild curves increased the accuracy of these predictions, particularly, for PT curves. These classifications were done by novice observers with no clinical scoliosis background. We speculate that the method would be more accurate when used by experienced clinicians, and this prediction will be tested as part of our future research. Some of the curves on the boundaries (eg. TL) may be easier to identify for an

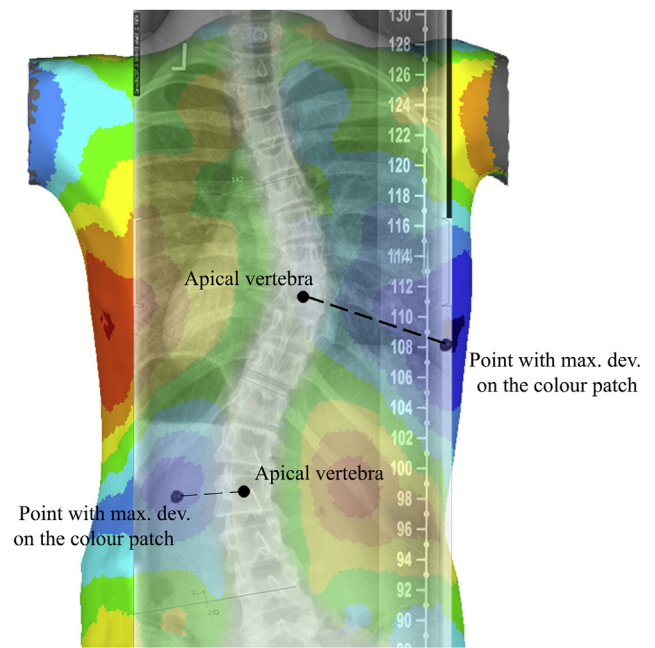


Fig. 5. The deviation color map of a patient with AIS with superimposed corresponding x-ray.

experienced clinician with a greater understanding of the underlying anatomy. A similar classification has been reported in which 97 patients who were candidates for surgery were analyzed using cross-sections of the torso. Although both mild and moderate curves were excluded from their analysis, only 72.2% of curves were correctly classified into three groups: major thoracic, double and triple, and lumbar major curves [31].

The ST measurement  $h_{ST}$  was able to predict the height of the curve apex using a regression model. The height of the maximum deviation on the DCM was lower than the actual curve apex as indicated by the resulting prediction model and by the majority of results lying above the bisector line (Fig. 3A, B). This relationship differs between T-TL curves and L curves, with the difference between  $h_{ST}$  and  $h_r$  being larger for T-TL curves, where the vertebrae are connected to the ribs (Fig. 5). The lateral deformation in the thoracic spine is transferred to the torso through the ribs, whereas in the lumbar section the vertebrae are surrounded with soft tissues, which may mask a portion of the deformity particularly for small curves [25,32]. The height of curve apex is an important parameter in design of personal braces, because it is the region that requires most in-brace correction and corresponds to where compensatory force should be applied to the torso surface. It was found that  $h_r$  was predicted for 24 test subjects within an average of 17 mm and 13 mm for T-TL curves and L curves, respectively. These values are smaller than the height of one vertebra [25] in this population and therefore represent errors of prediction clinically minor in importance.

Excluding mild curves improved the  $R^2$  values in the regression models for both T-TL and L curves. For patients

with a Cobb angle greater than 25° (where bracing is recommended), the  $h_{ST}$  parameter has a significant correlation with respect to the vertical location of the apical vertebra. The location of  $h_{ST}$  and pattern of color patches in the DCM may be useful clinically for both brace design and brace adjustments.

Curve severity was predicted with 73% accuracy for T-TL curves. Although 75% of moderate L curves were correctly diagnosed (Fig. 4), half of the mild and severe L curves were misidentified, especially when they were a part of double curves. This may be due to the small sample size for L curves, or an interconnected effect of asymmetry in the T-TL region and the surface deformity in the L section. With a double curve the prominent deviation in the upper back (section 2 or 3, Fig. 1) dominates the asymmetry analysis. Since such a curve would be in the opposite direction as the lumbar curve in Section 1, it may overshadow the relatively small deviation in the lumbar region of the DCM. Additional work is needed to increase the number of double curves analyzed and study the interconnected effect of T-TL and L curves.

The ST parameters were very accurate when distinguishing moderate or severe curves from mild curves in both the T-TL (95% accuracy) and L (90% accuracy) regions. This analysis can be used when following a patient over time to identify progression from mild scoliosis, typically requiring only observation, to moderate or severe scoliosis requiring intervention such as bracing. An increase in the curve severity identified on the DCM could be used to alert the physician of a progression so they can take required action to adjust the treatment or request an x-ray for further investigation.

In the future, the proposed asymmetry analysis will be tested for its ability to detect greater than 5° curve progression over time in patients with AIS. In the clinic, an increase of 5° or more is considered progression of the deformity [33]. Previous indicators yielded at best partial results and were limited by inter- and intraobserver variability [33–35].

The long-term goal of our work is to monitor the curves so that our model can identify mild curves that would transition to moderate or severe curves. However, in our current work, 3/57 of T-TL and 2/20 of L moderate and severe curves were incorrectly identified as mild. This corresponds to 5% and 10% for the T-TL and L curves, respectively. Although this is a small percentage, our future work will analyze these particular cases. In particular, we will correlate our results with the body mass index (BMI) to see if these cases are related to a high BMI that is preventing the ST model from detecting the severity of the curves.

Asymmetry of the torso associated with scoliosis results from a multivariable relationship between the torso and the spine shape and is influenced by the alignment of the spine, ribcage, trunk rotation, body fat, morphometry, and posture [12,30]. Previous attempts to relate torso surface geometry with the underlying spinal deformity have relied on a series of indices [21,26,27,31] and have been limited in their

clinical success. The spectrum of deformities associated with scoliosis cannot be fully captured by a discrete number of indices. The method presented here uses the entire torso surface and both a visual and quantitative representation of the asymmetry to better capture the torso deformity. This will enable clinicians to better predict the underlying spinal deformity from the torso surface with the aim of replacing some x-ray films with noninvasive ST images. The 3D nature of the asymmetry analysis presented here can also supplement current monitoring techniques to include measures of cosmetic appearance.

**Research Ethics Committee Approval:** Ethics approval from the Human Research Ethics Board has been obtained for this study.

## Funding Sources

The authors would like to gratefully acknowledge the sources that helped to fund this project, including the Scoliosis Research Society (SRS), the Women and Children Health Research Institute (WCHRI), and the Natural Sciences and Engineering Research Council of Canada (NSERC).

## References

- [1] Rogala EJ, Drummond DS, Gurr J. Scoliosis: Incidence and natural history. A prospective epidemiological study. *J Bone Joint Surg* 1978;60:173–6.
- [2] Robinson EF, Wade WD. Statistical assessment of two methods of measuring scoliosis before treatment. *Can Med Assoc J* 1983;129: 839–41.
- [3] Kittleston AC, Lim LW. Measurement of scoliosis. *Am J Roentgenol Radium Ther Nucl Med* 1970;108:775–7.
- [4] Reamy BV, Slakey JB. Adolescent idiopathic scoliosis: review and current concepts. *Am Fam Physician* 2001;64:111–6.
- [5] Cobb RJ. *Outline for the study of scoliosis. Instructional Course Lectures, American Academy of Orthopaedic Surgeons*, 5. St Louis, MO: CV Mosby; 1948. p. 261–75.
- [6] Hill DL, Berg DC, Raso VJ, et al. Evaluation of a laser scanner for surface topography. *Stud Health Technol Inform* 2002;88:90–4.
- [7] Ardran GM, Coates R, Dickson RA, et al. Assessment of scoliosis in children: Low dose radiographic technique. *Br J Radiol* 1980;53: 146–7.
- [8] Ronckers CM, Doody MM, Lonstein JE, et al. Multiple diagnostic X-rays for spine deformities and risk of breast cancer. *Cancer Epidemiol Biomarkers Prev* 2008;17:605–13.
- [9] Don S. Radiosensitivity of children: potential for overexposure in CR and DR and magnitude of doses in ordinary radiographic examinations. *Pediatr Radiol* 2004;34(Suppl 3):S167–72.
- [10] Doody MM, Lonstein JE, Stovall M, et al. Breast cancer mortality after diagnostic radiography: Findings from the U.S. scoliosis cohort study. *Spine* 2000;25:2052–63.
- [11] Hoffman DA, Lonstein JE, Morin MM, et al. Breast cancer in women with scoliosis exposed to multiple diagnostic x rays. *J Natl Cancer Inst* 1989;81:1307–12.
- [12] Goldberg CJ, Kalisz M, Moore DP, et al. Surface topography, Cobb angles, and cosmetic change in scoliosis. *Spine* 2001;26:E55–63.
- [13] Pratt RK, Burwell RG, Cole AA, Webb JK. Patient and parental perception of adolescent idiopathic scoliosis before and after surgery in comparison with surface and radiographic measurements. *Spine* 2002;27:1543–50.



- [14] Ajemba PO, Durdle NG, Hill DL, Raso VJ. A torso-imaging system to quantify the deformity associated with scoliosis. *Instrument Meas IEEE Trans* 2007;56:1520–6.
- [15] Moreland MS, Pope MH, Wilder DG, et al. Moire fringe topography of the human body. *Med Instrum* 1981;15:129–32.
- [16] Thometz JG, Lamdan R, Liu XC, Lyon R. Relationship between Quantec measurement and Cobb angle in patients with idiopathic scoliosis. *J Pediatr Orthop* 2000;20:512–6.
- [17] Theologis TN, Fairbank JC, Turner-Smith AR, Pantazopoulos T. Early detection of progression in adolescent idiopathic scoliosis by measurement of changes in back shape with the integrated shape imaging system scanner. *Spine* 1997;22:1223–7.
- [18] Tredwell SJ, Bannon M. The use of the ISIS optical scanner in the management of the braced adolescent idiopathic scoliosis patient. *Spine* 1988;13:1104–5.
- [19] Turner-Smith AR, Harris JD, Houghton GR, Jefferson RJ. A method for analysis of back shape in scoliosis. *J Biomech* 1988;21:497–509.
- [20] Hackenberg L, Hierholzer E, Potzl W, Gotze C, Liljenqvist U. Rasterstereographic back shape analysis in idiopathic scoliosis after posterior correction and fusion. *Clin Biomech* 2003;18:883–9.
- [21] Jaremko JL, Poncet P, Ronsky J, et al. Estimation of spinal deformity in scoliosis from torso surface cross sections. *Spine* 2001;26:1583–91.
- [22] Pazos V, Cheriet F, Song L, Labelle H, Dansereau J. Accuracy assessment of human trunk surface 3D reconstructions from an optical digitizing system. *Med Biol Eng Comput* 2005;43:11–5.
- [23] Ovadia D, Bar-On E, Fragniere B, et al. Radiation-free quantitative assessment of scoliosis: a multi center prospective study. *Eur Spine J* 2007;16:97–105.
- [24] Minguez MF, Buendia M, Cibrian RM, et al. Quantifier variables of the back surface deformity obtained with a noninvasive structured light method: evaluation of their usefulness in idiopathic scoliosis diagnosis. *Eur Spine J* 2007;16:73–82.
- [25] Stokes IA, Moreland MS. Concordance of back surface asymmetry and spine shape in idiopathic scoliosis. *Spine* 1989;14:73–8.
- [26] Suzuki N, Inami K, Ono T, Kohno K, Asher MA. Analysis of posterior trunk symmetry index (POTSI) in scoliosis. Part 1. *Stud Health Technol Inform* 1999;59:81–4.
- [27] Ajemba PO, Kumar A, Durdle NG, Raso VJ. Quantifying torso deformity in scoliosis. *Medical Imaging 2006: Image Processing. Proceedings of the SPIE* 6144:1608–1616.
- [28] Ajemba P, Durdle N, Hill D, Raso J. Classifying torso deformity in scoliosis using orthogonal maps of the torso. *Med Biol Eng Comput* 2007;45:575–84.
- [29] Komeili A, Westover L, Parent E, Moreau M, El-Rich M, Adeeb S. Surface topography asymmetry maps categorizing external deformity in scoliosis. *Spine J* 2014;14:973–83.
- [30] Ajemba PO, Durdle NG, Hill DL, Raso VJ. Validating an imaging and analysis system for assessing torso deformities. *Comput Biol Med* 2008;38:294–303.
- [31] Seoud L, Adankon MM, Labelle H, Dansereau J, Cheriet F. Prediction of scoliosis curve type based on the analysis of trunk surface topography. *Biomedical Imaging: From Nano to Macro, 2010 IEEE International Symposium on* 2010:408–11, <http://dx.doi.org/10.1109/ISBI.2010.5490322>
- [32] Scutt ND, Dangerfield PH, Dorgan JC. The relationship between surface and radiological deformity in adolescent idiopathic scoliosis: effect of change in body position. *Eur Spine J* 1996;5:85–90.
- [33] Lonstein J, Carlson J. The prediction of curve progression in untreated idiopathic scoliosis during growth. *J Bone Joint Surg* 1984;66:1061–71.
- [34] Peterson LE, Nachemson AL. Prediction of progression of the curve in girls who have adolescent idiopathic scoliosis of moderate severity. Logistic regression analysis based on data from the brace study of the scoliosis research society. *J Bone Joint Surg Am* 1995;77:823–7.
- [35] Duval-Beaupere G, Lamireau T. Scoliosis at less than 30 degrees. Properties of the evolutivity (risk of progression). *Spine* 1985;10:421–4.